GEOPHYSICAL RESEARCH LETTERS, VOL. 23, NO. 22, PAGES 3251-3254, NOVEMBER 1, 1996

A comparison of self-consistent kinetic and quasi-MHD simulations: Application to a dipolarizing field reversal

Sandra C. Chapman and Chris G. Mouikis[1]
Space and Astrophysics Group, University of Warwick, UK

Abstract. Self consistent one dimensional hybrid code (particle ions, massless electron fluid) simulations are used to examine the possible structure and evolution of a dipolarizing field reversal in the near earth geotail. Here, we run the simulations in both the ion kinetic (hybrid) limit, where the ion moments and the electromagnetic fields are all well resolved on ion Larmor scales, and the quasi- MHD limit, where all ion trajectories are still fully resolved but the ion moments are taken, and the electromagnetic fields are advanced on spatial scales larger than the gyroradii of the ions. One simulation selfconsistently includes the ion current and density resolved on ion Larmor scales whereas the other does not; both simulations have sufficient bandwidth to well resolve all the low frequency wave modes expected from kinetic (in the hybrid case) or 2 fluid (in the quasi-MHD case) theory. It is shown that the evolution of the electromagnetic field and ion pressure tensor are markedly different in the two cases. The results suggest that the selfconsistent quasi- MHD solution obtained in this way cannot be obtained from a coarse graining of the full kinetic (hybrid) selfconsistent solution.

1. Introduction

Selfconsistent simulations are now widely used to study magnetospheric boundary layers and structures. The set of equations used, and hence the solution obtained, depends on the a priori choice of the spatio- temporal scales to be represented. Another approach, used for example in the geotail, is to integrate large numbers of single particle trajectories in prescribed fields that are obtained from either global empirical models [e.g. *Ashour-Abdalla et al.*, 1994] or from MHD simulations [e.g. *Joyce et al.*, 1995]. This has the advantage that the region where ions are accelerated is connected to a global system, but the disadvantage of non selfconsistency in the sense that the the bulk plasma moments (number density n, ion current $\mathbf{J_i}$, ion pressure $\mathcal{P}_i$) of the evolving ion $f(\mathbf{v})$ do not contribute to the fields on ion Larmor scales. Here we examine this a priori assumption: that solutions of this type can be adequately obtained without resolving selfconsistency on ion Larmor scales. The simple example used here is localized "dipolarization" in the near earth geotail. The initial condition of the simulation is out of equilibrium: the magnetic field reverses smoothly and symmetrically in an isotropic plasma. Subsequently the magnetic reversal relaxes (dipolarizes) as there is insufficient parallel plasma pressure to maintain equilibrium. Hybrid code simulations of this system [*Richardson and Chapman*, 1994] show that ions are accelerated giving a non isotropic ion pressure tensor and a cross tail (GSE y directed) magnetic field component is generated which is also seen in hybrid simulations of rotational discontinuities [e.g. *Lin and Lee*, 1993].

2. Simulation Details

The hybrid scheme used here [*Terasawa et al.*, 1986] represents the ion $f(\mathbf{v})$ with an ensemble of computational particles that follow trajectories prescribed by the Lorentz force law; the change in positions and velocities of these computational particles are resolved on scales determined by the simulation timestep Δt. At each timestep the ion number density and current density $n_i, \mathbf{J}_i$ are obtained by taking moments of the computational particle ensemble onto the simulation grid and are hence resolved at the grid spacing Δx (and for numerical stability a Courant condition is also satisfied i.e. $\Delta x > c\Delta t$ where c is the velocity of the fastest wave mode in the simulation). The fields are then advanced on the simulation grid using quasi- neutrality, the "massless" electron fluid momentum equation where the inertial term has been neglected (and with $P_e = nkT_e$, T_e constant), and Maxwell equations at low frequency (displacement current term neglected). At the next timestep the fields on the grid are then extrapolated to the particle positions to advance the particle trajectories.

The two simulation runs shown here have identical bulk plasma parameters and time resolution (in terms of the ion Larmor period) differing only in the spatial resolution of the simulation grid. In the hybrid case, $\Delta x \ll R_{gi}$ the thermal ion gyroradius in the background field: the fields are advanced using currents resolved on scales $\ll R_{gi}$ and the ions experience changes in the fields as they move several Δx in a single gyration about the field. In the MHD scale case, $\Delta x > R_{gi}$: the field advance does not include spatial variations in the current on ion Larmor scales and the ions experience little change in the fields as they remain within a single grid cell Δx as they gyrate about the field, only being carried from one cell to the next by field aligned or drift motion of the guiding centre. In both cases the bandwidth of the simulation is sufficient to well resolve the expected low frequency modes (e.g. *Krauss-Varban et al.* [1994]) which are not identical in the kinetic and the quasi- MHD limits. The physical parameters for both simulations are: $v_{inflow} = 0.1V_{a,x}$, ($V_{a,x}$ is the Alfven speed in $\hat{x}$) $\beta_i = 0.1$, $T_e = 0.1T_i$, $n = 0.2cm^{-3}$, $B_x = 20nT$ and $B_z = 2nT$. The code

[1]Now at Max-Planck-Institut für Aeronomie, Germany

Paper number 96GL02845.
0094-8534/96/96GL-02845$05.00

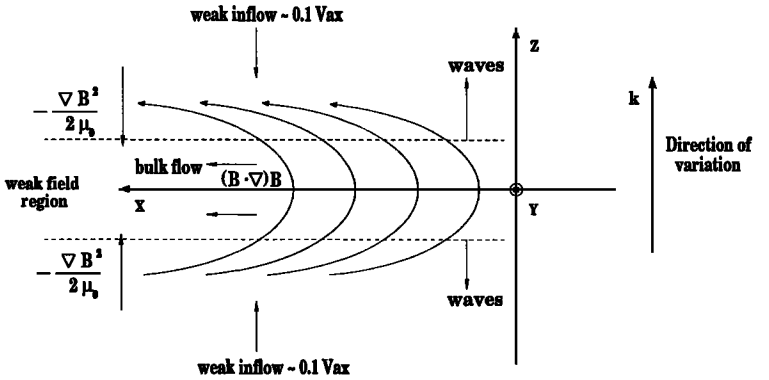

Figure 1. Geometry of the simulation.

parameters are: $\Delta z = 1/10R_{gi}$ $(0.03c/w_{pi})$ in the hybrid case and $\Delta z = 2R_{gi}$ $(0.65c/w_{pi})$ in the MHD scale case; $\Delta t = 1/1630\tau_{gi}$ in both cases; the simulation box has 4096 grid cells in the hybrid case and 512 in the MHD scale case; 100 computational particles per cell are used in both cases and the simulations have a bandwidth of $0.055 < k < 111.6(c/\omega_{pi})^{-1}$ (hybrid case) and $0.019 < k < 4.8(c/\omega_{pi})^{-1}$ (MHD scale) with $0.1 < \omega < 800\Omega_{ci}^{-1}$ in both cases.

The initial and boundary conditions are identical, the ion distribution is initially isotropic, has weak inflow towards the centre $z = z_0$ and is spatially uniform, $B_x = B_{x0}tanh((z-z_0)/L)$, $(L = 1.95c/\omega_{pi})$ $B_y = 0$, the electric field then evolves selfconsistently. The boundaries are wave and particle absorbing. The geometry of the one dimensional simulation is shown in Figure 1. All scalars and vector components are retained but vary in the one space direction $(\hat{z})$ directed across the reversal, and time. The field threading the reversal at $t = 0$, B_z, is constant $(\nabla \cdot \mathbf{B} = 0)$ in this one dimensional geometry. All waves then propagate in $\pm\hat{z}$, and the ∇B^2 magnetic pressure acts along $\pm\hat{z}$ to contain the plasma in the weak field region at the centre of the reversal, whereas the $(\mathbf{B} \cdot \nabla)\mathbf{B}$ curvature force acts perpendicular to the direction of variation and accelerates the plasma. The electric field in the simulation frame is:

$$\mathbf{E} = -\mathbf{v_i} \wedge \mathbf{B} + \frac{\mathbf{J} \wedge \mathbf{B}}{ne} - \frac{\nabla \cdot \mathcal{P}_e}{ne} + \frac{C_{ei}}{ne} \qquad (1)$$

for single ion and electron fluids in the hybrid limit and

$$\mathbf{E} = -\mathbf{v} \wedge \mathbf{B} + \eta\mathbf{J} \qquad (2)$$

for MHD. In the MHD limit $\mathbf{v} \equiv \mathbf{v_i}$ in (2) so $\mathbf{E}$ differs by a term of order $\mathbf{J} \wedge \mathbf{B}/ne$ in the hybrid and MHD cases. We will see however that the principal differences in the two solutions are characterised by differences in $\mathbf{v_i} \wedge \mathbf{B}$, which is large compared with $\mathbf{J} \wedge \mathbf{B}/ne$.

3. Results

The bulk parameters and ion phase space for the two simulations are shown in Figure 2 (hybrid) and Figure 3 (MHD scale) plotted versus direction of variation across the reversal z. In both cases the central 512 cells of the simulation box are shown corresponding to 46 R_{gi} $(14.4c/\omega_{pi})$ for the hybrid run and 1026 R_{gi} $(329.6c/\omega_{pi})$ for the MHD scale run. The parameters are shown for $t = 9.8\tau_{gi}$, sufficiently late in the simulations to correspond to the "post escape" phase in the hybrid solution [*Richardson and Chapman*, 1994] when the ions escape from the reversal and can be seen to be moving towards the boundaries.

Electromagnetic Fields: From early times in the hybrid solution a bipolar B_y component evolves as the

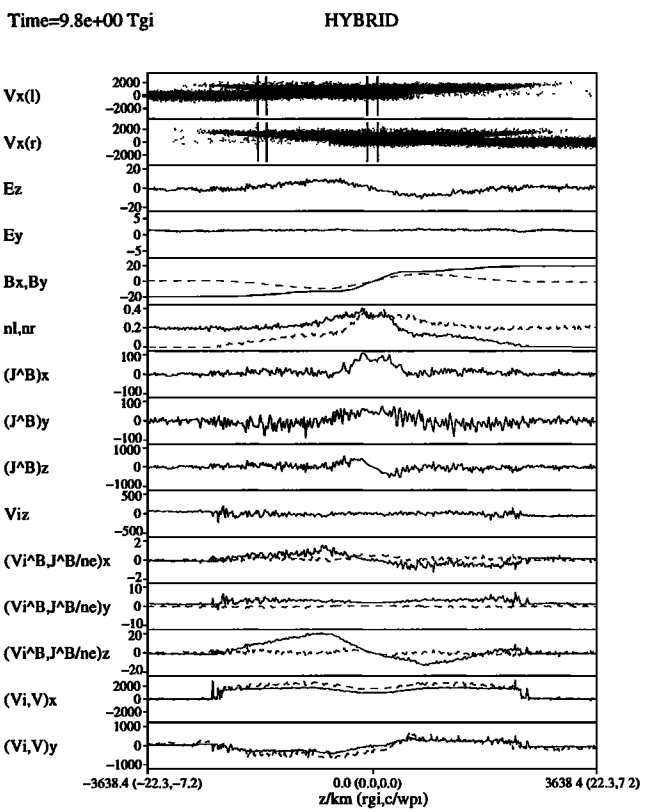

Figure 2. From top to bottom: V_x phase space for left and right entering ions (kms^{-1}) (lines indicate where $f(\mathbf{v})$ is taken for Figures 4, 5), E_z, E_y (mVm^{-1}), B_x (solid) and B_y (dashed) (nT), number density of the left (solid) and the right (dashed) entering ions (cm^{-3}), normalized $\mathbf{J} \wedge \mathbf{B}$ components $(.10^3)$, z component of the ion bulk velocity (kms^{-1}), $\mathbf{V_i} \wedge \mathbf{B}$ (solid lines) and $\mathbf{J} \wedge \mathbf{B}/ne$ (dashed lines) components (mV/m), bulk velocity x and y components V_i (solid) and V (dashed) (kms^{-1}).

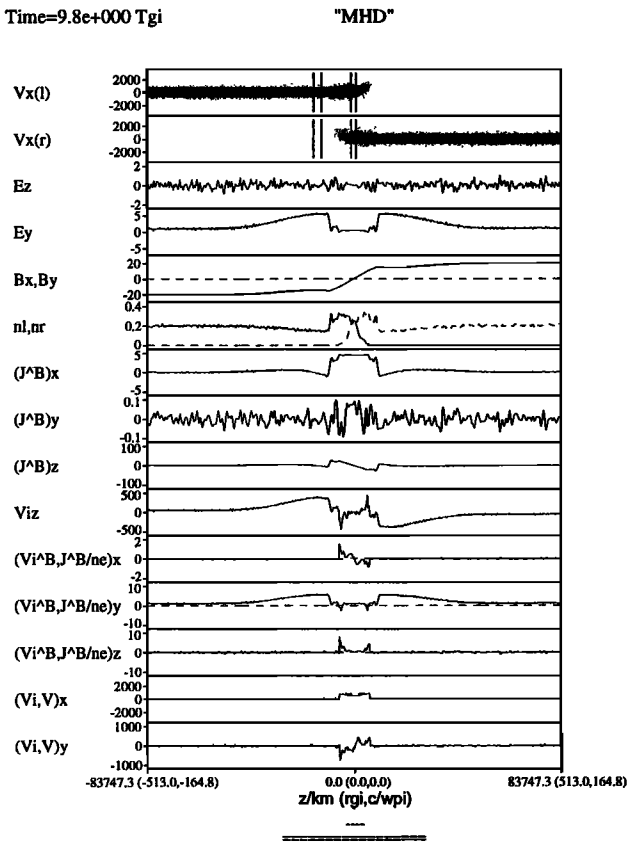

Figure 3. As for Figure 2 but for the MHD scale case. The double dashed bar indicates the full size of the hybrid case simulation box, the single dashed bar indicates the size of the region shown in Figure 2.

magnetic field rotates out of the x, z plane across the reversal. The MHD scale solution does not develop significant B_y i.e. the magnetic field remains in the x, z plane. In both cases the B_x component reverses sharply in a central region where the density is strongly enhanced and is slightly depressed in a region just outside. This depression in B_x just outside the reversal is physically different in the two solutions, however. In the hybrid case, B_x is depressed as the local density is increased by the ions escaping from the reversal. In the MHD scale case, the local density is decreased in this region, accompanied by an increase in the v_z component of bulk velocity into the reversal and an accompanying signature in $E_y = -v_z B_x$. This compressional mode has an analogue in the hybrid solution in the form of a fast mode wavepacket which is generated at early times and which has moved out of the simulation box. A bipolar E_z (with corresponding $(\mathbf{v_i} \wedge \mathbf{B})_z$) evolves in the hybrid case over a region occupied by the escaping ions. The E_x component (not shown) is within the noise levels of the simulations in both cases. The terms $\mathbf{v_i} \wedge \mathbf{B}$ and $\mathbf{J} \wedge \mathbf{B}/ne$ are plotted on the same scales for comparison and at this stage in the simulations the $\mathbf{v_i} \wedge \mathbf{B}$ term dominates, that is, the $\mathbf{J} \wedge \mathbf{B}/ne$ term in equation (1) does not account for the differences in $\mathbf{E}$ in the hybrid and MHD scale solutions.

Bulk Plasma Acceleration: The components of $\mathbf{J} \wedge \mathbf{B}$ are also shown on Figures 2-3 (normalized to x magnetic pressure/ion inertial length). In both cases this term is significant only in the central reversal region so that it does not act on the ions once they have escaped from this region in the hybrid case. The z component then corresponds to ∇B^2 in (1) and acts to contain the plasma in the reversal and the x (and in the hybrid case, also y) components correspond to the curvature force that accelerates the plasma. Although the magnitude of $\mathbf{J} \wedge \mathbf{B}$ is about 20 times smaller in the MHD scale case, in physical units the width of the central reversal at this time is about 20 times larger, hence the rate of delivery of momentum from the relaxing B field to to the plasma over the entire simulation box is the same in both simulations.

Ion Distribution Functions: The difference in the ion dynamics in the two cases can be seen in the top

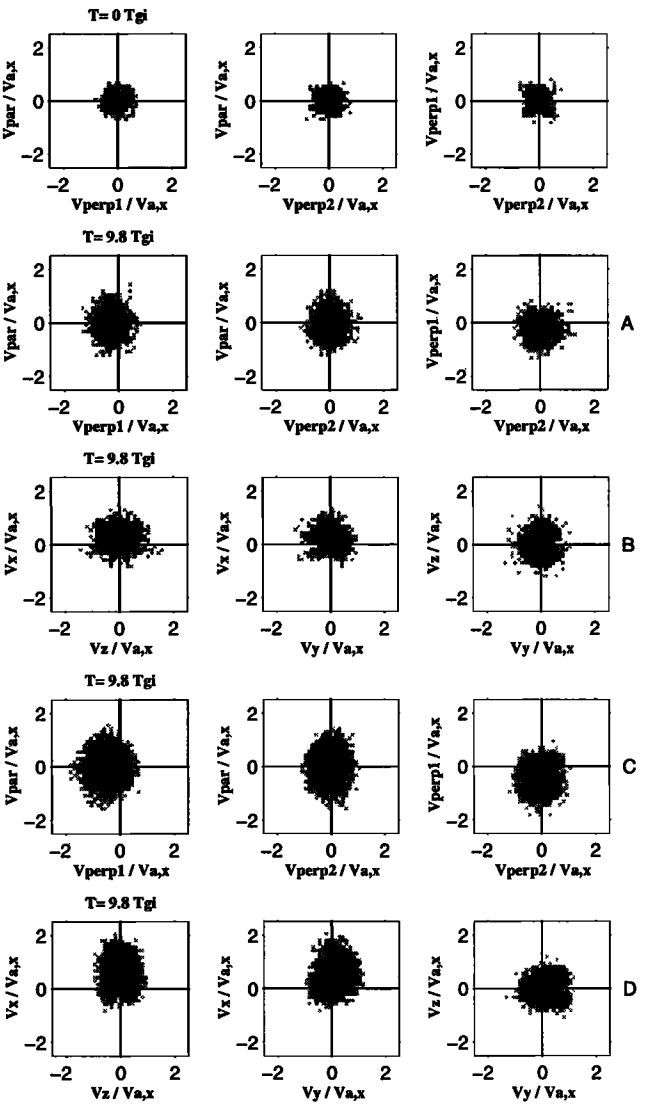

Figure 4. Ion $f(\mathbf{v})$ in the reversal centre for the MHD scale case (A, B) and hybrid scale case (C, D). Vpar, Vperp1, Vperp2 $(v_\parallel, v_{\perp 1}, v_{\perp 2})$ form a right handed orthogonal cartesian coordinate system (see text). Vx, Vy, Vz correspond to GSE. Va,x is the Alfven speed in the B_x field. The logarithmic grey scale ranges from 1 computational particle per pixel (light grey) to $\sim$ 50 computational particles per pixel (black).

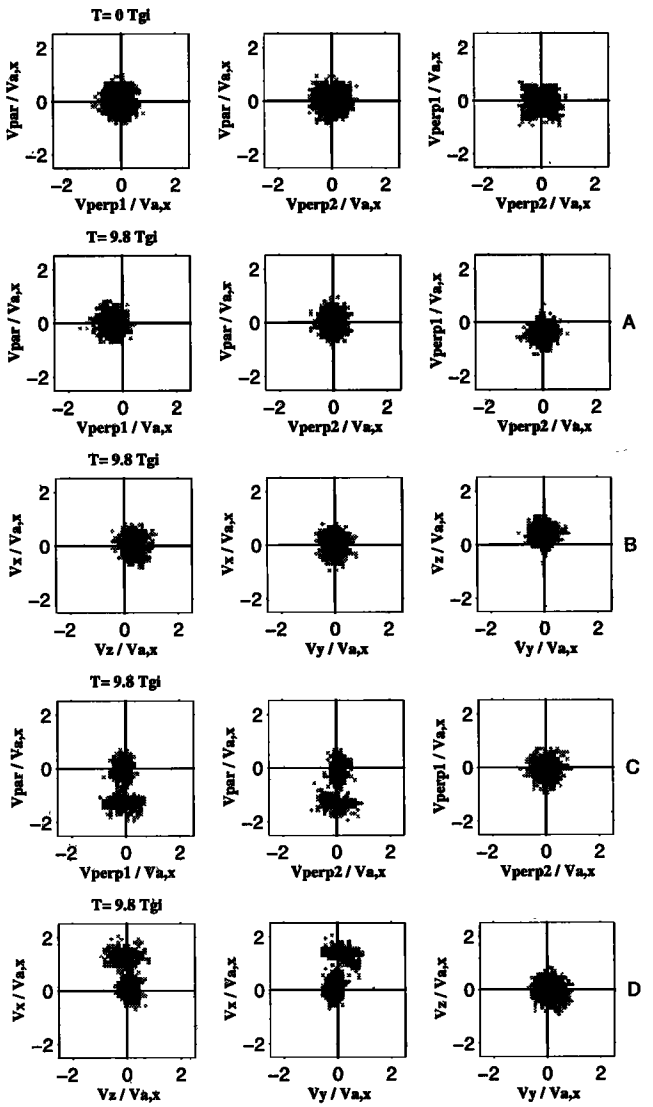

Figure 5. Ion $f(\mathrm{v})$ from a region outside the reversal for the MHD scale case (A, B) and the hybrid scale case (C, D), same format as Figure 4.

panel of Figures 2 and 3 which shows v_x of individual computational particles versus z. Distribution functions have been plotted for the regions marked with the vertical lines, inside (Figure 4) and outside (Figure 5) of the reversal. These show projections of the distribution in the $v_{\|}, v_{\perp 1}$ plane and the $v_{\perp 1}, v_{\perp 2}$ plane, at $t = 0$ and at the time shown in Figures 2 and 3 (with $v_{\|}$ directed along the local $\mathbf{B}$, $v_{\perp 1}$ lies in the x, z plane and $v_{\|}, v_{\perp 1}, v_{\perp 2}$ form a right handed cartesian coordinate system). The $t \neq 0$ distributions are also shown plotted in v_x, v_y, v_z space, corresponding to the approximately GSE coordinate system of the simulation (see Figure 1). From Figure 4 we see that inside the reversal the MHD scale solution (A,B) is characterised by an isotropic ion distribution throughout the run which is heated to maximum thermal speed $\sim V_{ax}$ and which has a cross field bulk motion of $\sim 0.5 V_{ax}$ in the $+x$ direction. In the hybrid case (C, D) the ion $f(\mathrm{v})$ is heated more strongly along the field and has a cross field drift in both x and y which is higher also $\sim 0.5 - 1 V_{ax}$. Just outside of the reversal (Figure 5) in the MHD scale case (A, B) the ion $f(\mathrm{v})$ is almost unchanged from the input distribution, it has the same temperature and a cross field drift, in $+z$ (this distribution is taken in the region where there is significant E_y). In the hybrid case (C, D) the escaping ions can be clearly seen, moving out of the reversal along the field with up to $\sim 2 V_{ax}$. In a sufficiently large simulation box this unstable distribution would ultimately thermalize.

4. Conclusions

For a simple dipolarizing reversal, we have found that important features of the hybrid solution cannot be "coarse grained" to yield the MHD scale solution. It should be stressed that the details of these results will differ for different systems, or in more realistic geometries (allowing quantities to vary in three space coordinates). Nevertheless this example demonstrates the importance of resolving selfconsistently on ion Larmor scales a plasma configuration that energizes the ions. This has relevance in particular for recent studies of ion energization and predictions of the ion distribution function in the geotail that involve integrating large numbers of test particle trajectories in prescribed fields obtained on MHD scales (i.e. larger than ion gyroscales), either from phenomenological field models or from the output of MHD codes.

Acknowledgments. This work was conducted whilst C.G.M. was supported by PPARC and S.C.C. was in part supported by a Nuffield Foundation Research Fellowship.

References

Ashour-Abdalla, M., L. M. Zelenyi, V. Peroomian and R. L. Richard, Consequences of magnetotail ion dynamics, *J. Geophys. Res.*, 99, 14891, 1994

Joyce, G., J. Chen, S. Slinker, D. L. Holland, and J. B. Harold, Particle energization near an X line in the magnetotail based on global MHD fields, *J. Geophys. Res.*, 100, 19167, 1995

Krauss-Varban, D., N. Omidi, and K. B. Quest, Mode properties of low-frequency wave: Kinetic theory versus Hall-MHD, *J. Geophys. Res.*, 99, 5987, 1994

Lin, Y., and L. C. Lee, Structure of the Dayside Reconnection Layer in Resistive MHD and hybrid Models, *J. Geophys. Res.*, 98, 3919, 1993

Richardson, A., and S. C. Chapman, Self consistent one-dimensional hybrid code simulations of a relaxing field reversal, *J. Geophys. Res.*, 99, 17391, 1994

Terasawa, T., M. Hoshino, J. I. Sakai, and T. Hada, Decay Instability of Finite-Amplitude Circularly Polarized Alfven Waves: A Numerical Simulation of Stimulated Brillouin Scattering, *J. Geophys. Res.*, 91, 4171, 1986

Space and Astrophysics Group, Univ. of Warwick, UK

(Received April 11, 1996; revised July 9, 1996;
accepted September 11, 1996.)